Interaction of Frontside Halo CMEs

X.P. Zhao
W.W. Hansen Experimental Physics Laboratory, Stanford University

Abstract

Recent research shows that fast moving CMEs can collide and/or merge with slower moving previously CMEs in the outer corona. The CME interaction has important implications for space weather prediction based on frontside halo CMEs.

We first derive the necessary and sufficient conditions for two successive frontside halo CMEs to be able to interact with each other in the outer corona and interplanetary space inside the Earth orbit, then determine the propagation velocity and angular size for five frontside halo CMEs between April 5 and 11, 2001 using the conical model of halo CMEs, and finally select the pair of CMEs that is satisfied with the necessary and sufficient conditions and examine their interplanetary counterpart using in situ data observed by ACE near 1 AU. The colliding CMEs (20010409_15:42 and 20010410_05:30) produce two forward shocks at 20010411_13:02 and 20010411_15:18 followed by a 30-hour interval without any characteristics of Parker spiral field configuration.

— The AGU Fall Meeting, December 10 – 14, 2001, San Francisco

1. Introduction

Long-wavelength radio and white-light observations on WIND/WAVES and SOHO/LASCO have shown evidence for interactions between CMEs in the outer corona and interplanetary medium. The shock process is suggested to be one of such interactions. The shock strengthening when the preexisting shock ahead of the fast CME plows through the core of the preceding slow CME causes intense continuum-like radio emission following an interplanetary type II burst. The duration of the radio enhancement is consistent with transit time of the CME-driven shock through the core of slow CME. As a consequence of this interaction, the core velocity of the slow CME changed its both direction and speed significantly (Gopalswamy et al., ApJ., 548L91, 2001). The reconnection between CMEs' internal magnetic field is supposed to be another kind of CME interactions. Both the reconnection and the formation of a new shock due to collision between CMEs may accelerate nonthermal electrons responsible for a new class of radio emission. There was no type II radio burst preceding the nonthermal emission in such interaction. This CME interaction may seriously affect the propagation of CMEs (Gopalswamy et al., GRL, in press, 2001).

These interactions between CMEs have important implications for space weather prediction based on halo CMEs: some of the false alarms could be accounted for by CME interactions.

As shown in the next section, in order to predict the occurrence of the interactions between successive halo CMEs we need to know the propagation velocity and the angular size of the halo CMEs in addition to the onset time of the halo CMEs. In Section 3 we examine the five halo CMEs between April 5 and 11, 2001 using the conical model (Zhao et al., submitted, 2001) to determine which pair of halo CMEs is able to interact with each other. The associated ACE data are also examined to see its characteristics near the Earth orbit. In the last section we summarize the results.

2. Criteria for occurrence of CME interaction

The speed of the later CME, v_i, faster than that of the earlier CME, v_{i-1}, is a necessary condition for the occurrence of the interaction between two successive CMEs, but it is not a sufficient condition.

Many coronal mass ejections (CMEs) observed near the solar limb propagate almost radially beyond the first few solar radii, and their angular widths remain nearly constant while propagating through the corona. Assuming that these characteristics hold true for halo CMEs that originate far from the limb, the halo CME propagation may be described using a simple model of a CME as a cone (Zhao et al., 2001), and the necessary and sufficient conditions for the occurrence of CME interaction can be derived as follows

$$v_i > v_{i-1}, \tag{1}$$

$$\hat{v}_i - \hat{v}_{i-1} < (hfwd_i + hfwd_{i-1})/n, \tag{2}$$

$$\triangle t_{i(i-1)} = \frac{v_i(t_i - t_{i-1})}{v_i - v_{i-1}} < \triangle t_{iEarth}. \tag{3}$$

Symbols $\hat{v}_i$ and $hfwd_i$ in Equation (2) denote the propagation direction and the angular width of the later halo CME, n is any number greater than 1. In Equation (3), t_i denotes the onset time of the later halo CME, $\triangle t_{i(i-1)}$ is the time interval needed for the later CME overtaking the earlier slow CME, and $\triangle t_{iEarth}$ is the time interval needed for the later CME arriving at the Earth orbit if there were no the earlier slow CME. $\triangle t_{iEarth}$ can be inferred based on the propagation speed projected in the plan of the sky (v_{sky} published at http://cdaw.gsfc.nasa.gov/) and the experienced relationship between $\triangle t_{iEarth}$ and v_{sky} (Gopalswamy et al., GRL, 27, 145, 2000). Equations (1) and (2) are the necessary and sufficient conditions for two successive CMEs to be able to interact with each other, and Equation (3) ensures that the CME interaction takes place in the interplanetary space within 1 AU so that it may have influence on the space weather.

3. The five halo CMEs between April 5 and 11, 2001

We have developed a conical model of halo CMEs for determining the geometric and kinematic properties of halo CMEs (Zhao et al., submitted, 2001). By matching the observed halos at a series of times with the modeled halos for a series of radial distances the propagation velocity and the half of the angular size can be obtained.

Figures 1 and 2 display modeled halos (black circles) overplotted on observed bright halos for the frontside full halo CMEs on 20010409_15:42 and 20010410_05:30 denoted by 'Apr09' and 'Apr10'.

The time-distance scatter plot and their constant speed and constant acceleration fitting can be obtained using the series of time and radial distance in Figures 1 and 2 (see the top panels in Figures 3 and 4). The speed and acceleration at verious heights can also be inferred (see the bottom panels in Figures 3 and 4).

Table 1 lists the propagation velocity and the half of the angular width obtained for five frontside halo CMEs between April 5 and 11, 2001.

Table 2 shows the results used in Equations (1), (2) and (3). Only one pair of CMEs (Apr09 and Apr10) is satisfied with the three conditions.

Figure 5 shows in situ observations made by ACE from April 5 to April 15. The onset time of the five CMEs is indicated using symbol '*'. The vertical dotted lines denote the interplanetary shocks observed by SOHO/CELIAS/MTOF. The four vertical dashed lines and the adjacent CME names indicate the inferred times $\triangle t_{iEarth}$ when the CME arrives at the Earth if there was no adjacent earlier CME. The red lines in panels of By (Bx) and Longitude are obtained using observed Bx (By) and proton speed based on Parker's spiral model. The computed red curves match the observed one very well between 20010407_02 UT and 20010408_10 UT and between 20010412_22 UT and 20010413_04 UT, suggesting that they are solar wind from coronal holes. The shock on April 7 is thus caused by stream-stream interaction, rather than the CME on April 5. The significant difference between the observed and computed curves occurs in three time intervals, around Apr09, Apr11_22–Apr12_06, and Apr13_12–Apr14_08. The plasma β in Apr11_22–Apr12_06 and Apr13_12–Apr14_08 have extremely low values less than 0.05. The solar wind disturbance in Apr13_12–Apr14_08 and the shock ahead of it is caused by the CME Apr11. The two green dotted lines are supposed to be generated by the frontside full halo CMEs of Apr09 and Apr10. The three green solid lines mark the boundary of the colliding CMEs. This interaction generated a big geomagnetic storm as shown by the Dst panel.

Figure 6 shows the interplanetary magnetic field and plasma properties from April 5 to April 15. The interaction interval contains two parts. The first part have the proton speed, density temperature, total magnetic field and the plasma β significantly higher than the second part.

4. Summary

• The necessary and sufficient conditions for successive frontside halo CMEs to be able to interact with each other before arriving the Earth have been derived. The conditions depend on the propagation velocity and the angular width as well as the onset time of the halo CMEs.

• The conical model of halo CMEs may be used to determine the propagation velocity and the angular width of frontside halo CMEs and to judge whether or not a pair of successive halo CMEs is able to interact with each other and whether or not the CME interaction will be affecting space weather.

• The frontside halo CMEs observed at 20010409_15:42 UT and 20010410_05:30 UT are satisfied with the necessary and sufficient conditions, and generate two successive forward shocks at 20010411_13:02 and 20010411_15:18. The interplanetary counterpart of the colliding CMEs contains two parts. The first part has the proton speed, density, temperature, magnetic field and plasma β significantly higher than what in the second part.

• Halo CMEs often show the magnetic field configuration of flux ropes. Whether or not the orientation of the central magnetic field of one CME is basically parallel to the other may be used to determine whether or not the CME interaction involves in magnetic reconnection. It is possible to predict the type of CME interactions if we can determine the orientation of the CMEs from solar observations.

Acknowledgements

Many thanks to Nat Gopalswamy for allowing me to download his reprint and preprint on coronal mass ejection interactions from the web page of the Center for Solar Physics and Space Weather. The ACE IMF and SWEPAM data, as obtained from NSSDC's OMNI dataset, were used in this analysis.

Table 1: The propagation velocity and the half of angular width

HCME_i date	Onset time	hfwd_i deg.	$\hat{v}_i$ deg.	v_i km/s	v_{sky} km/s	$\triangle t_{iEarth}$ hours
Apr05	17:06:05	25	$\phi = -30, \theta = 6$	850	1390	35.4
Apr06	18:42:05	37	$\phi = -9, \theta = -7$	580	1270	39.2
Apr09	15:42:05	30	$\phi = 7, \theta = -4$	1275	1192	42.1
Apr10	05:30:00	34	$\phi = 10, \theta = -12$	2080	2411	19.0
Apr11	13:31:48	35	$\phi = 8, \theta = -7$	760	1103	46.0

Table 2: Examining the necessary and sufficient conditions

HCME_i	v_i km/s	$(\mathrm{hfwd}_i + hfwd_{i-1})/2$ deg.	$\hat{v}_i - \hat{v}_{i-1}$ deg.	$\triangle t_{i(i-1)}$ hours	$\triangle t_{iEarth}$ hours
Apr05	850				
Apr06	580	31.0			
Apr09	1275	33.5	16.27	57.6	42.1
Apr10	2080	32.0	8.5	13.5	19.0
Apr11	1103	34.5			

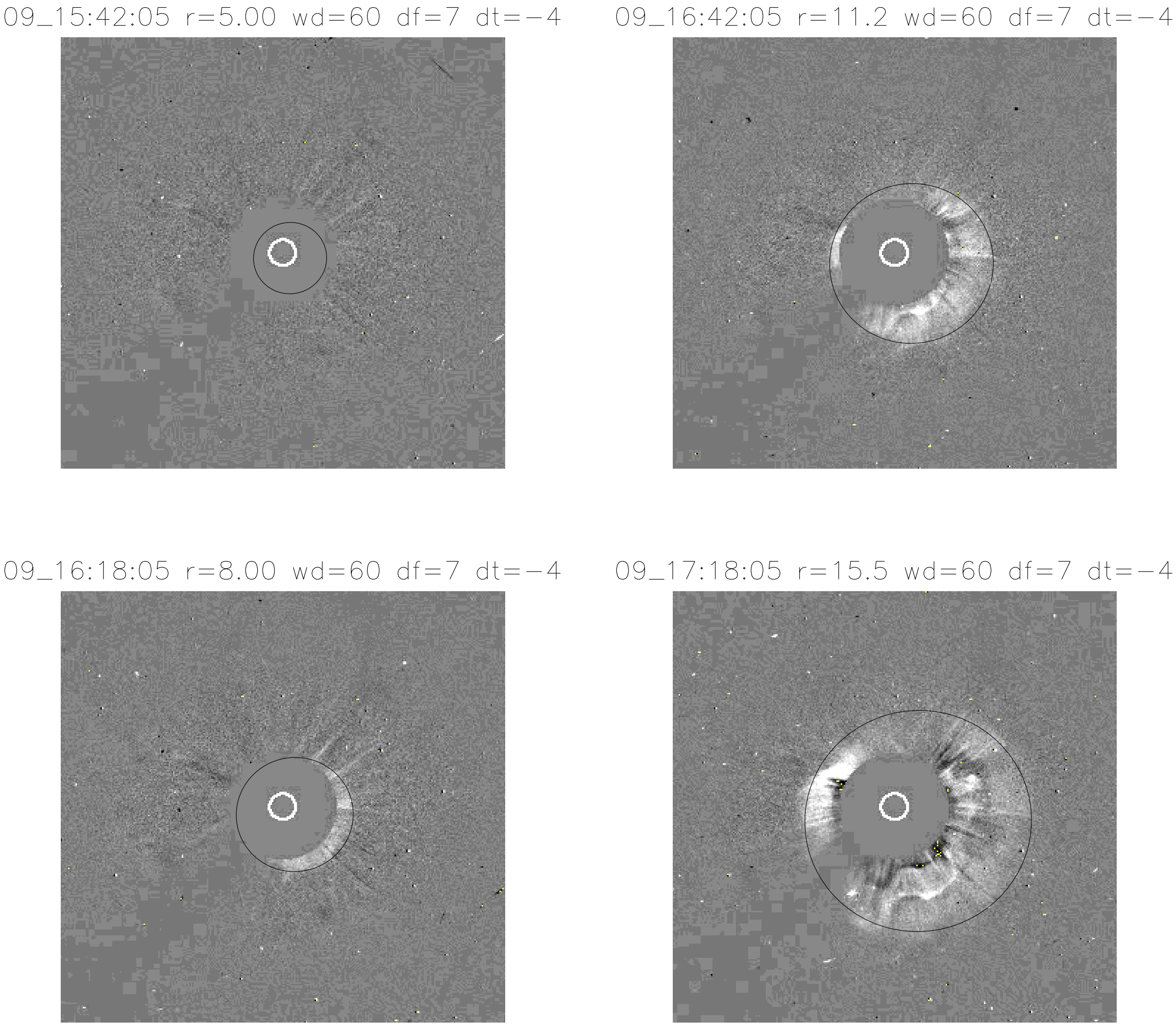

Fig. 1.— Comparison of predicted halos (dark circles) for April 9, 2001 halo CME at different radial distances with observed halos at a series of times. The time, radial distance (r), angular size (wd), longitude (df) and latitude (dt) are shown on the top of each panel. The small white circle denotes the solar disk

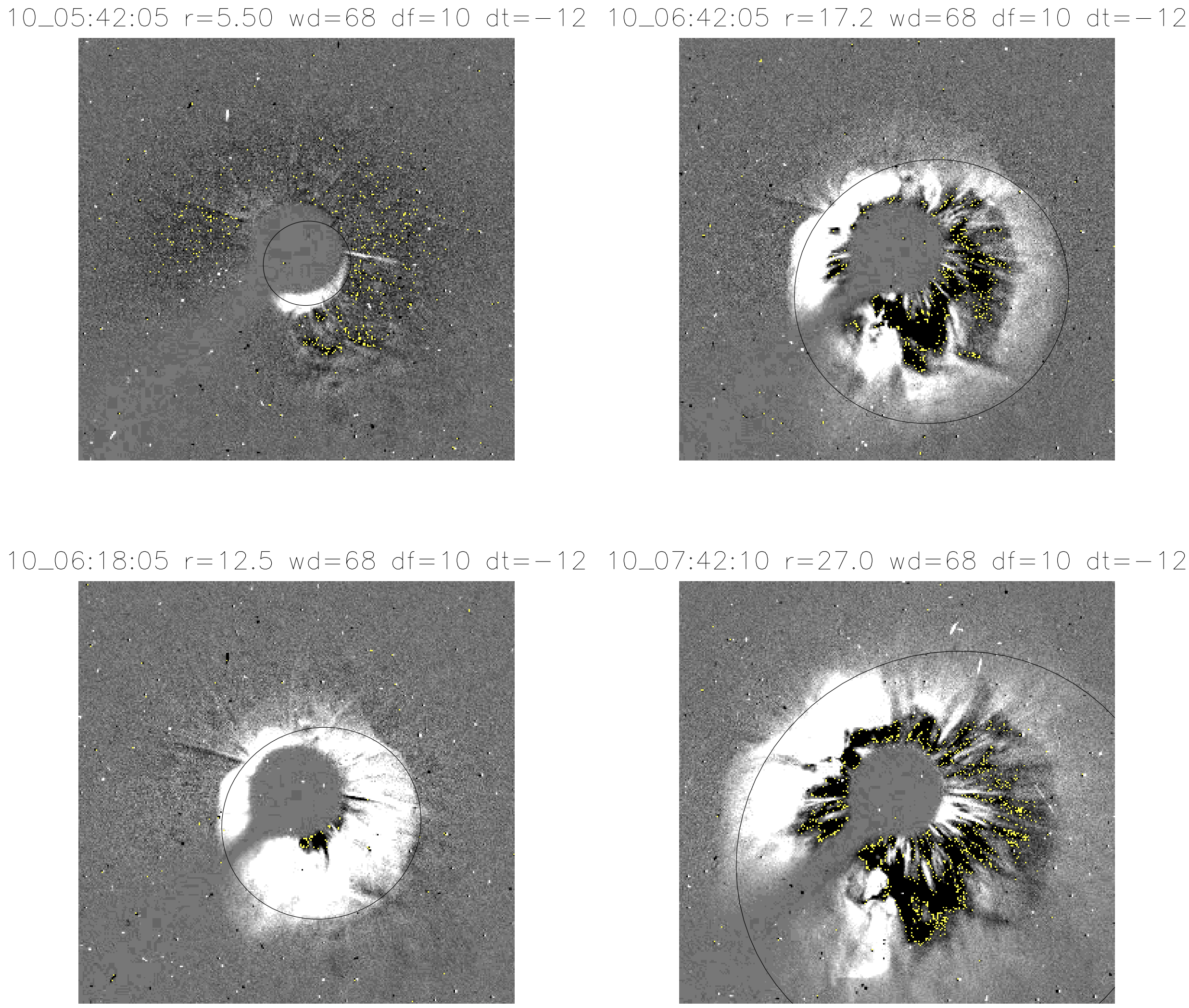

Fig. 2.— The same as Figure 1 but for April 10, 2001 halo CME

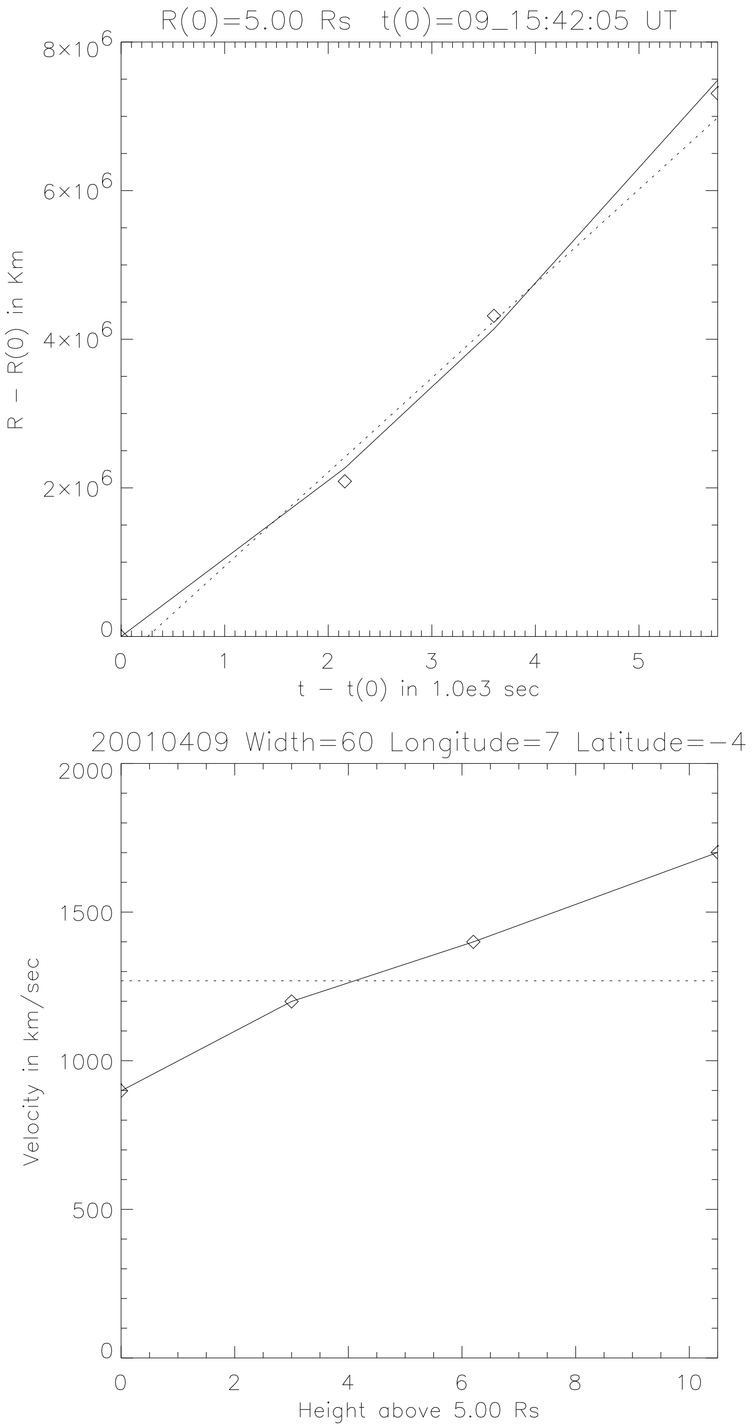

Fig. 3.— The plot (the top panel) of the inferred series of time and radial distance as shown in the top of each panel of Figure 1. Here R(0) and t(0) are shown on the top of the top panel. The dotted and solid lines are fits obtained using the Downhill Simplex Fitting technique, assuming constant speed and constant acceleration, respectively.

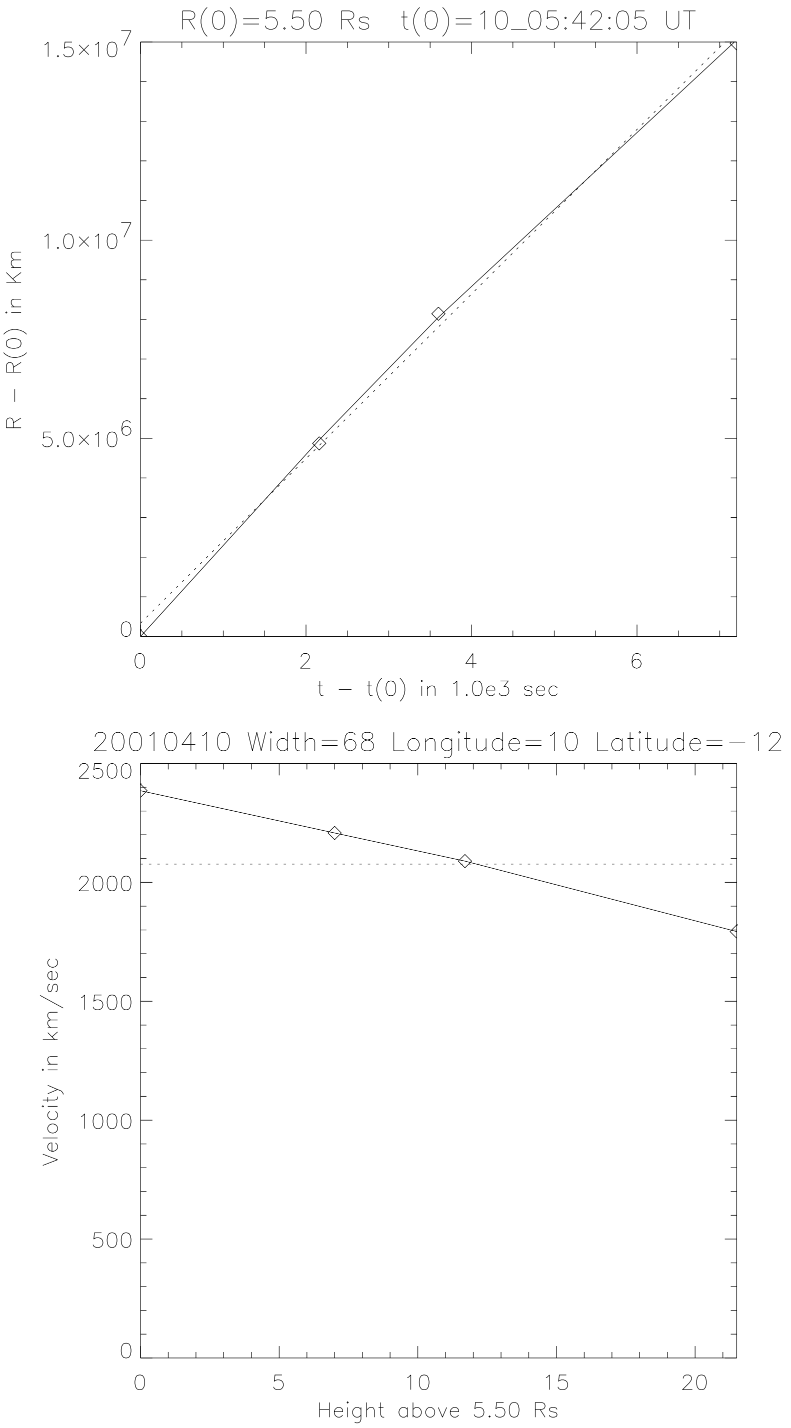

Fig. 4.— The plot (the top panel) of the inferred series of time and radial distance as shown in the top of each panel of Figure 2. Here R(0) and t(0) are shown on the top of the top panel. The dotted and solid lines are fits obtained using the Downhill Simplex Fitting technique, assuming constant speed and constant acceleration, respectively.

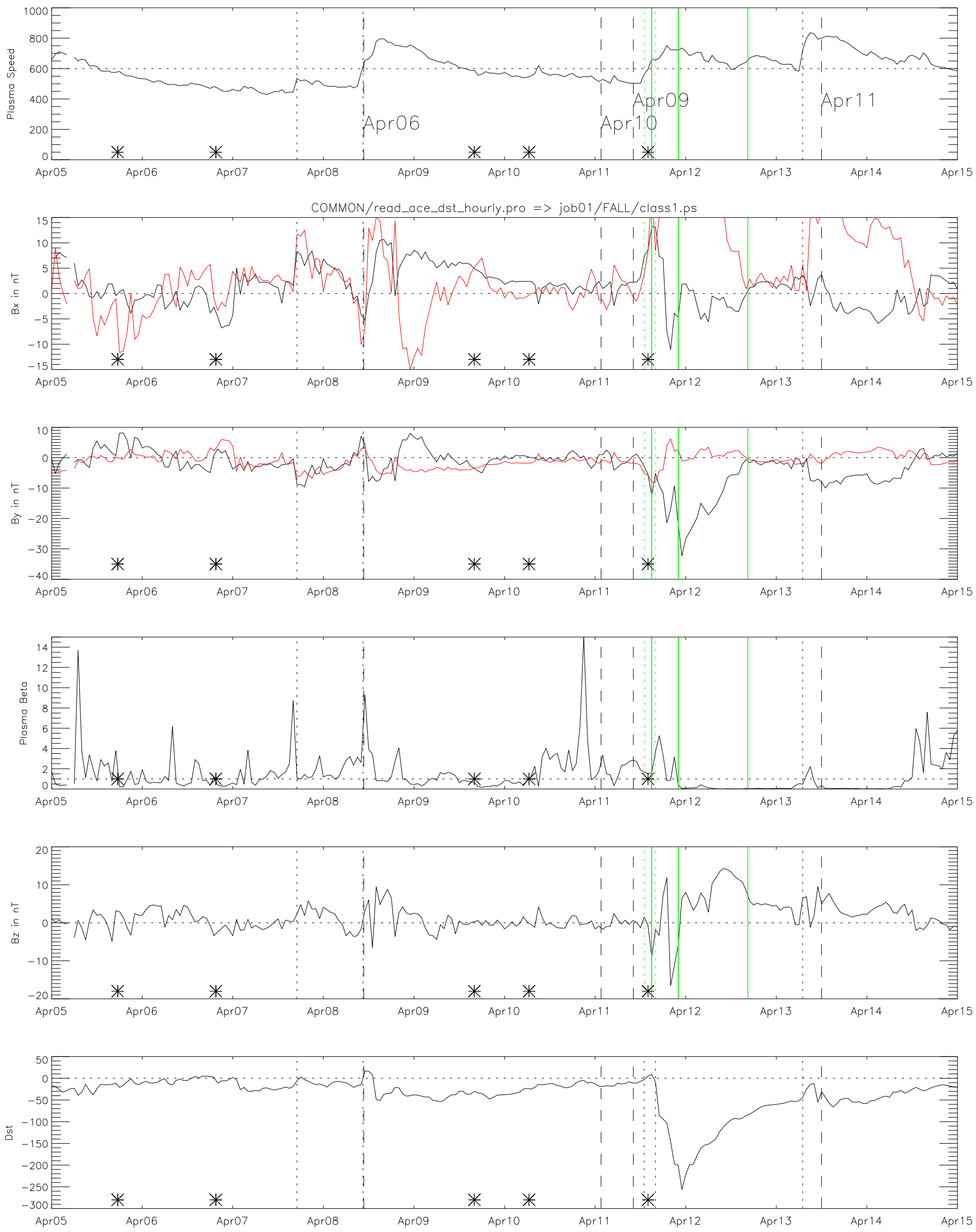

Fig. 5.— ACE observations of proton speed, IMF radial and east-west components, plasma β, IMF north-south component and the geomagnetic disturbance index Dst. The symbol '*' denotes the onset time of five frontside halo CMEs between April 5 and 11, 2001. The vertical dotted lines denote the interplanetary shocks observed between April 7 and 13, 2001. The dashed lines with the onset date of the CME denote the time when the CME arrives at the Earth if there was no adjacent earlier CME. The red line in Bx (By) panel is obtained using observed By (Bx), proton speed and Parker's spiral formulae. The green dotted lines are supposed to be generated by the CMEs Apr09 and Apr10 bordered by three green solid lines.

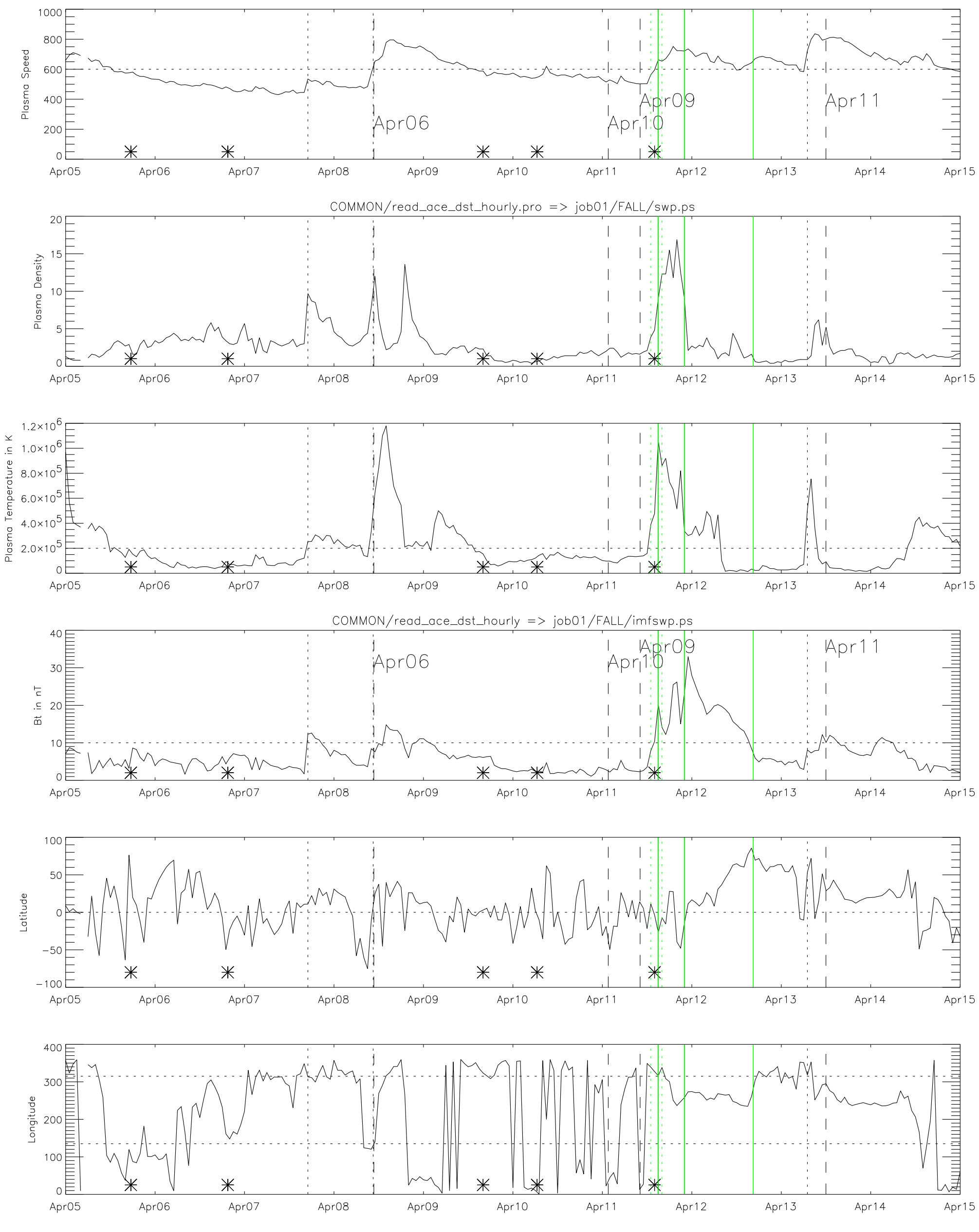

Fig. 6.— ACE observations of interplanetary magnetid field and solar plasma, showing the characteristics of the interaction between CMEs of Apr09 and Apr10.